Egypt. J. Chem. **Vol. 63**, No. 11 pp. 4235 - 4241 (2020)

Egyptian Journal of Chemistry

http://ejchem.journals.ekb.eg/

Analysis of Electronic, Raman and UV-vis Spectra for $Zn_{11}Se_{11}$, $Zn_{11}S_{11}$, and Ternary Alloys $Zn_{11}S_nSe_{11-n}$(n= 1-11) A DFT/TDDFT Study

Hussein H. Abed[a*], Hayder M. Abduljalil[a], Mudar A. Abdulsattar[b]

[a] *Department of Physics, College of Science, University of Babylon, Iraq.*

[b] *Ministry of Science and Technology, Baghdad, Iraq.*

Abstract

$Zn_{11}Se_{11}$, $Zn_{11}S_{11}$, and ternary alloys from $Zn_{11}S_nSe_{11-n}$ (n = 1 - 11), with cubic structures represented by nanostructures called tetramantane, have been studied theoretically by investigating the electronic properties, Raman and UV-vis spectra. LUMO and HOMO levels were observed to change with the number of the sulfur atoms. The (HOMO - LUMO) gap for $Zn_{11}Se_{11}$ (2.377205eV) increased with the sulfur atoms. $Zn_{11}S_8Se_3$ have an energy gap (3.061305eV) less than others ternary alloys. The calculated energy gap of $Zn_{11}S_{11}$ (3.597374eV) is in a high agreement with experimental value (3.6 eV). Raman spectra for ternary alloys $Zn_{11}S_nSe_{11-n}$ content peaks result from the connection of ($Zn_{11}Se_{11}$+$Zn_{11}S_{11}$) peaks, $Zn_{11}Se_{11}$ has peak at 260.42 cm^{-1} shifts from the experimental value by a small deviasion which is produced due to the confinement effect. UV-vis spectra for ternary alloys shifted to a higher energy level with the increase in the number of sulfur atoms and dramatically close to $Zn_{11}S_{11}$ UV-vis spectrum except $Zn_{11}S_8Se_3$ has λ_{max} at 342 nm. These nanostructures are suitable to be used in different applications such as lenses, photoelectronic devices, solar energy, and biosensors. DFT/TDDFT at the B3LYP level with SDD basis functions is used. All the calculations are completed using the Gaussian 09 program.

Keywords: Dimondoids; Ternary alloys; DFT/TDDFT.

1. Introduction

Nanomaterials are characterized by a large surface area to volume ratios and quantum confinement effect, therefore, their physicochemical and biological properties are different from bulk form. For an instance, the nanomaterials exhibit an increase in the energy gap, high interfacial reactivity, and improved surface chemical reactivity toward external adsorbents. Therefore, these are reasons for these nanomaterials to be used in many practical and biomedical applications [1-3]. Currently, there is a significant theoretical and experimental interest in chalcogenides due to their various applications in science and technology [4-9]. Zinc sulfide and zinc selenide at the nanoscale regime having beneficial optical and electrical properties; therefore, it is used in different fields such as mid-infrared laser applications, photocatalysts, and sensors [10-12]. The formation of ternary alloys of varying concentrations offers the possibility of obtaining a material having the ability to regulate optical and electrical properties [13]. Ternary alloys from (Zn, S, and Se) atoms are considered as a promising material in the construction of biomedical labels, lenses and optically controlled switches due to high occupied molecular orbital (HOMO), lower unoccupied molecular orbital (LUMO) levels, and lattice parameters variation with the compositions [14,15]. Cubic structure of ZnSe and ZnS at the nanoscale were represented by $Zn_{11}Se_{11}$ and $Zn_{11}S_{11}$ nanostructures. To get ternary alloy ($Zn_{11}S_nSe_{11-n}$), selenium atoms were replaced by sulfur atoms for (n= 1-11). The aim of this work is to investigate the electronic, Raman spectra, and UV-vis spectra for

*Corresponding author e-mail: hakimhussein.2017@gmail.com.;
Receive Date: 24 July 2019, Revise Date: 28 August 2019, Accept Date: 23 March 2020
DOI: 10.21608/ejchem.2019.15197.1923

these structures by using Gaussian 09 program, density functional theory at the B3LYP level with SDD basis function. UV-vis spectra were calculated by using time-dependent density functional theory.

2. Computational Details

Diamondoids and wurtzoids nanostructures are suggested to represent zincblende and wurtzite structures at the nanoscale regime [16-19]. Small stoichiometric Zn_nS_n Zn_nSe_n, Cd_nS_n, and Cd_nSe_n structural clusters have been established previously by others [20]. In the present work, ZnSe and ZnS cubic diamondoids were used to represent ZnSe and ZnS nanocrystals. Tetramantane of $Zn_{11}S_{11}$ and $Zn_{11}S_{11}$ were used as a representative of these diamondoids due to its appropriate base size which enabled reasonable computer calculation times while the size of the these structured were increased. Fig. 1 and Fig. 2 show an example of these optimization calculations for tetramantane $Zn_{11}S_{11}$.

Fig.1:Tetramantane $Zn_{11}S_{11}$after optimization.

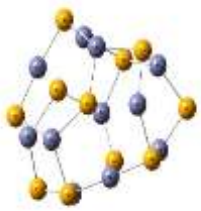

Fig.2:Tetramantane $Zn_{11}Se_{11}$ after optimization.

Ternary alloys from Zn, S and Se atoms with compositions $Zn_{11}S_nSe_{11-n}$ (n = 1 - 11) include $Zn_{11}SSe_{10}$, $Zn_{11}S_2Se_9$, $Zn_{11}S_3Se_8$, $Zn_{11}S_4Se_7$, $Zn_{11}S_5Se_6$, $Zn_{11}S_6Se_5$, $Zn_{11}S_7Se_4$, $Zn_{11}S_8Se_3$, $Zn_{11}S_9Se_2$, and $Zn_{11}S_{10}Se$ are shown in Fig. 3.

The present work flow consisted of three stages:

1- Structures were optimized to get the preferred configurations.
2- The vibrational properties were calculated and compared with experimental measurements.
3- UV-vis spectra were calculated to determine the possibility of optical applications.

DFT/TDDFT at the B3LYP level with SDD basis function was used to calculate the properties by Gaussian 09 program [21].

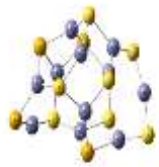

$Zn_{11}S_6Se_5$

$Zn_{11}S_7Se_4$

$Zn_{11}S_9Se_2$

$Zn_{11}S_{10}Se$

Fig.3: Ternery alloys of $Zn_{11}SSe_{10}$, $Zn_{11}S_2Se_9$, $Zn_{11}S_3Se_8$, $Zn_{11}S_4Se_7$, $Zn_{11}S_5Se_6$, $Zn_{11}S_6Se_5$, $Zn_{11}S_7Se_4$, $Zn_{11}S_8Se_3$, $Zn_{11}S_9Se_2$, and $Zn_{11}S_{10}Se$ after optimazation.

$Zn_{11}SSe_{10}$

$Zn_{11}S_2Se_9$

$Zn_{11}S_3Se_8$

$Zn_{11}S_4Se_7$

$Zn_{11}S_5Se_6$

$Zn_{11}S_6Se_5$

3. Results and discussion

3.1 Energy gap

All structures in this work have a size of a few nanometers; therefore, confinement effects are dominante and lead to size and shape-dependent electronic structure. Furthermore, as the size of the structure decreased, the surface effect increased producing changes in the density of the states and separation in the energy levels [22,23]. Fig .4 shows the relation between the energy gap as a function of increasing the number of sulfur atoms. $Zn_{11}Se_{11}$ has energy gap (2.377205 eV) which converged to the experimental value (2.7 eV) [24]. When the selenium atoms were replaced by the sulfur atoms a decrease in the HOMO and LUMO levels were observed and widening in the energy gaps were shown in Table 1. The ability to regulate the value of the energy gap by changing the number of selenium and sulfur atoms is significant and enabled different applications in photo-electronic devices and biosensor [14]. Table 1 shows that $Zn_{11}S_8Se_3$ has LUMO level lower than other ternary alloys structures, therefore, the energy gap dropped to (3.061305eV), and most stable form sulfur atoms formed from S_8 arranged in a very distinguishing crown-shaped cycle. The energy gap of $Zn_{11}S_{11}$ (3.597374eV) is in good agreement with experimental value (3.6 eV) [25]. This indicates the success of the proposed model and the method used.

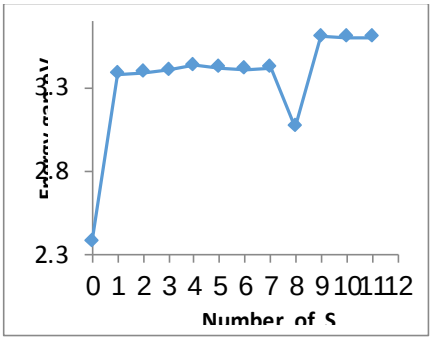

Fig. 4: Variations of the energy gap with S atom.

Table 1: The HOMO and LUMO levels, and energy gap.

Structures	HOMO eV	LUMO eV	Energy gap eV
$Zn_{11}Se_{11}$	-6.23826	-3.86105	2.377205
$Zn_{11}SSe_{10}$	-6.4233	-3.04198	3.381313
$Zn_{11}S_2Se_9$	-6.43636	-3.05015	3.386212
$Zn_{11}S_3Se_8$	-6.47364	-3.07137	3.402266
$Zn_{11}S_4Se_7$	-6.49623	-3.06675	3.429478
$Zn_{11}S_5Se_6$	-6.515	-3.09586	3.419138
$Zn_{11}S_6Se_5$	-6.53106	-3.12199	3.409069
$Zn_{11}S_7Se_4$	-6.56371	-3.14702	3.416688
$Zn_{11}S_8Se_3$	-6.68943	-3.62812	3.061305
$Zn_{11}S_9Se_2$	-6.75746	-3.156	3.601455
$Zn_{11}S_{10}Se$	-6.78657	-3.18838	3.59819
$Zn_{11}S_{11}$	-6.8029	-3.20553	3.597374

3.2 Raman spectra

The observed Raman shift is a direct measure of the information about the energies of molecular vibrations and rotations. The scattered radiation produced by the Raman effect is depended on the atoms or ions that constitute the molecule, the chemical bonds between them, the symmetry of the structure, and the physicochemical environment [26].

Raman spectrum for all studied structures are shown in Fig.5. The $Zn_{11}Se_{11}$ has a maximum peak at frequency of 260.42 cm^{-1} this represented LO mode which converges to experimental LO mode value of 250 cm^{-1} [27]. This calculation shows a clear shift of 10.42 cm^{-1} due to quantum confinement effect which is overriding the size property in this case. Replacing the selenium atoms by sulfur cased a shift in maximum peak indicating construct the ternary alloy from Zn, Se, and S atoms as shown in Table 2. The positions of peaks for ternary alloys with n=1,2,3,4,5,6,7 converge to LO mode of ZnS at 200 cm^{-1} [15], while ternary alloys with n=8,9,10 converge to LO mode for ZnSe at 250 cm^{-1}[28].

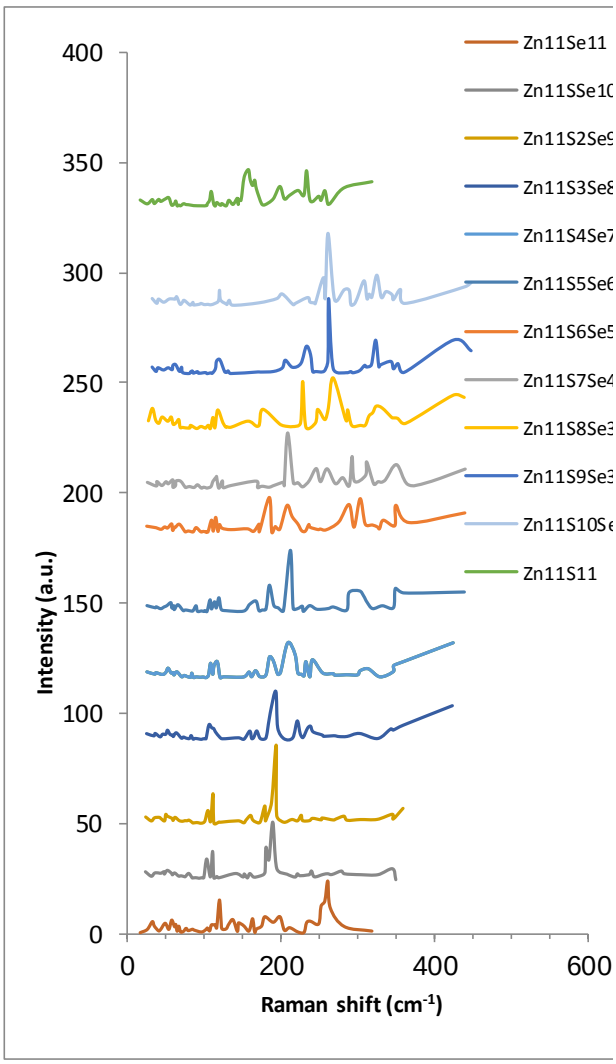

Fig.5: Raman spectra for structures.

Table 2: Maximum peaks for the Raman spectrum.

structures	Maximum peak (cm^{-1})
$Zn_{11}Se_{11}$	260.42
$Zn_{11}SSe_{10}$	188.86
$Zn_{11}S_2Se_9$	193.30
$Zn_{11}S_3Se_8$	192.78
$Zn_{11}S_4Se_7$	208.27
$Zn_{11}S_5Se_6$	211.79
$Zn_{11}S_6Se_5$	184.41
$Zn_{11}S_7Se_4$	208.23
$Zn_{11}S_8Se_3$	267.45
$Zn_{11}S_9Se_2$	261.49
$Zn_{11}S_{10}Se$	254.73
$Zn_{11}S_{11}$	258.43

3.3 UV-Visible spectra

Photons of ultraviolet and visible light are energetic enough to stimulate outer electrons to excite from HOMO to LUMO levels. The nanocrystals size approaches to Bohr radius, confinement, and surface (dangling bonds) induce changes in the energy level separation and produce an increase in the bandgap with the decrease in the size and the attendance of discrete energy levels near the band edges. Therefore, the semiconductor nanocrystal and ternary alloy have optoelectronic properties dependent on size, shape, composition, and doping. Fig. 6 shows the UV-vis spectra of the studied nanostructures. From Fig. 5 UV-vis spectrum for $Zn_{11}Se_{11}$ has a maximum peak at 420.8 nm (2.94 eV) and converge to experimental value of 2.7 eV [24]. The replacement of selenium atoms by sulfur gave rise to energy levels within the energy gap of the nanostructures because of the exciton relaxation into localized states reduces the overlap between the electron (e) and hole (h) wave functions. Thus, the maximum peaks shifted to higher energy and converged to 295.2 nm (4.2 eV) which is corresponding to ZnS experimental value of 3.6 eV [25, 28], as shown in Table 3. $Zn_{11}S_8Se_3$ has a maximum peak at 342 nm (3.6257eV) which is corresponding to the energy gap of 3.0613 eV.

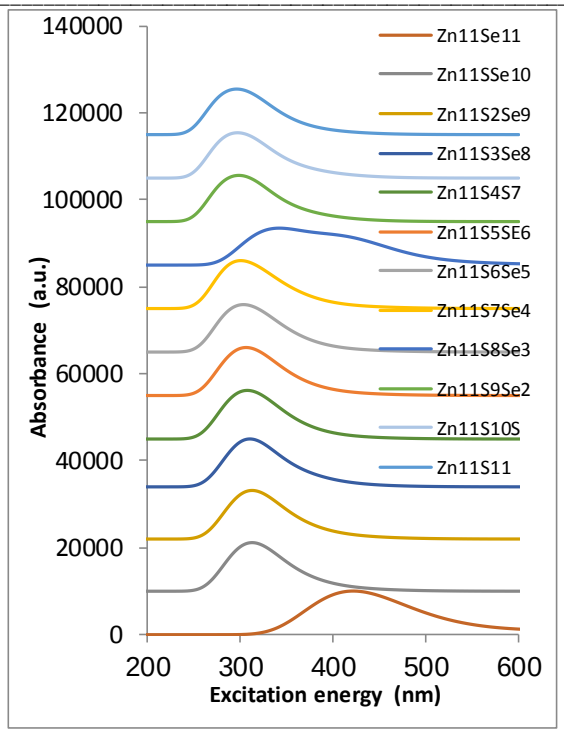

Fig.6: UV-vis spectra for structures.

Table 3: maximum peaks for the UV-vis spectra.

structures	UV-vis (λ_{max}) nm
$Zn_{11}Se_{11}$	420.8
$Zn_{11}SSe_{10}$	313.0
$Zn_{11}S_2Se_9$	312.0
$Zn_{11}S_3Se_8$	309.4
$Zn_{11}S_4Se_7$	306.6
$Zn_{11}S_5Se_6$	306.2
$Zn_{11}S_6Se_5$	302.4
$Zn_{11}S_7Se_4$	299.6
$Zn_{11}S_8Se_3$	342
$Zn_{11}S_9Se_2$	297.6
$Zn_{11}S_{10}Se$	296.4
$Zn_{11}S_{11}$	295.2

4. Conclusions

Dimondiods structures were implemented to represent the cubic structure at the nanoscale regime which gave results with good agreement with the published experimental measurement. Implemented tetramantane structures for zinc selenide $Zn_{11}Se_{11}$, zinc sulfide $Zn_{11}S_{11}$, were used to obtain ternary alloys $Zn_{11}S_nSe_{11-n}$ (n = 1 - 11), its nanostructures have HOMO-LUMO gap which increased with the increase of the concentrations of the sulfur atoms. The calculated energy gap of $Zn_{11}S_8Se_3$ is (3.061305 eV) which is lower than other studied structures because of the LUMO level. Raman spectra refer to construct ternary alloys from Zn, S, and Se because of the appearing of new peaks different from ZnSe and ZnS peaks, UV-Vis spectra of $Zn_{11}S_nSe_{11-n}$ (n = 1 - 11) shift to higher energy level with increased concentrations of sulfur atoms and converge to ZnS bandgap. Control of the value of bandgap by the changing the compositions of alloy serves as an important tool in different applications such as photoelectronic devices, and biosensor.

5. Conflicts of interest

There are no conflicts to declare.

6. Formatting of funding sources

There are no funding sources.

7. Acknowledgments

There are no acknowledgments.

8. References

1- Hashim A., Abduljalil H. M., and Ahmed H., Fabrication and Characterization of (PVA-TiO2)$_{1-x}$/ SiC_x Nanocomposites for Biomedical Applications, *Egypt. J. Chem.*, DOI: 10.21608/EJCHEM.2019.10712.1695, (2019).

2- Ahmed H. and Hashim A., Fabrication of PVA/NiO/SiC Nanocomposites and Studying their Dielectric Properties For Antibacterial Applications, *Egypt. J. Chem.*, DOI: 10.21608/EJCHEM.2019.11109.1712, (2019).

3- Ahmed H., Hashim A. and Abduljalil H. M., Analysis of Structural, Electrical and Electronic Properties of (Polymer Nanocomposites/ Silicon Carbide) for Antibacterial Application. *Egypt.J.Chem.* 62, 4. 1167 – 1176(2019).

4- Kumar D. S., Kashif M., Rethinasami V., Ravikumar B., Pandiarajan S. , Ayeshamariam A., Sivaranjani S., Bououdina M., and Ramalingam S. ,Synthesis and characterization

of zinc selenide (ZnSe) thin films electrodeposited on ITO and SnO_2 substrates. *Journal of Ovonic Research*, 10, 5. 175 – 184 (2014).

5- Boo B. H., Cho H., and Kang D. E., Ab initio and DFT investigation of structures and energies of low-lying isomers of Zn_xSe_x (x = 1–4) clusters. *Journal of Molecular Structure: Theochem*. 806, 77–83 (2007).

6- Azpiroz J. M., Matxain J. M., Infante I., Lopez X. and Ugalde J. M., A DFT/TDDFT study on the optoelectronic properties of the amine-capped magic $(CdSe)_{13}$ nanocluster. *Physical Chemistry Chemical Physics*, (2013).

7- Abed H. H., Abduljalil H. M., and Abdulsattar M. A., Structural, Optical and Humidity Sensitivity for CdSe Nanocrystalline Thin films. *J. Adv. Pharm. Edu. Res*., 8, 4. 52-31 (2018).

8- Abdulsattar M. A., Abduljalil H. M., and Abed H. H., Structure, Stability and Vibrational Properties of CdSe Wurtzite Molecules and Nanocrystals: A DFT Study. *Karbala International Journal of Modern Science*, 5, 119-125 (2019).

9- Thangam Y., Anitha R., and Kavitha B., Novel method to synthesize and characterize Zinc Sulfide Nanoparticles. *Int. Journal of Applied Sciences and Engineering Research*, 1, 2. (2012).

10- Saravanamoorthy S. N., Peter A. J. and Lee C. W., Optical peak gain in a PbSe/CdSe core-shell quantum dot in the presence of magnetic field for mid-infrared laser applications. *Chem. Phys*., 1–6.483–484 (2017).

11- Wang X., Xie Z., Huang H., Liu Z., Chen D. and Shen G., Gas sensors, thermistor and photodetector based on ZnS nanowires. *J. Mater. Chem*., 22. 6845, (2012).

12- Zhang F., Li C., Li X., Wang X., Wan Q., Xian Y., Jin L., and Yamamoto K., ZnS quantum dots derived a reagentless uric acid biosensor. *Talanta*, 68, 1353–1358 (2006).

13- Yang C.S., Hsieh Y.P., Kuo M.C., Tseng P.Y., Yeh Z.W., Chiu K.C., Shen J.L., Chu A.H.M., Chou W.C., and Lan W.H. ,Compressive strain-induced heavy hole and light hole splitting of $Zn_{1-x}Cd_xSe$ epilayers grown by molecular beam epitaxy. *Materials Chemistry and Physics*, 78, 602–607 (2003).

14- Chaudhari G.N., Manorama S. and Rao V.J., Deposition of $ZnS_{0.056}Se_{0.944}$ thin films on GaAs ((110)) substrates a new chemical growth technique. *Thin solid films*, 208, 243-246 (1992).

15- Makhavikou M., Parkhomenko I., Vlasukova L., Komarov F., Milchanin O., Mudryi A., Zhivulko V., Wendler E., Togambayeva A., and Korolik O., Raman monitoring of ZnSe and ZnS_xSe_{1-x} nanocrystals formed in SiO_2 by ion implantation. *Nuclear Inst, and Methods in Physics Research*, B, (2018).

16- Abdulsattar M.A., Molecular approach to hexagonal and cubic diamond nanocrystals. *Carbon Lett*. 16, 192–197 (2015).

17- Abdulsattar M.A. and Mohammed I.S., Diamondoids and large unit cell method as building blocks of InAs nanocrystals: a density functional theory study. *Comput. Mater*. Sci., 91, 11–14 (2014).

18- Abdulsattar M. A., GaN wurtzite nanocrystals approached using wurtzoids structures and their use as a hydrogen sensor: A DFT study. *Superlattices Microstruct*, 93, 163-170 (2016).

19- Abdulsattar M. A., Abduljalil H. M., and Abed H. H., Formation energies of CdSe wurtzoid and diamondoid clusters formed from Cd and Se atomic clusters. *Calphad*, 64, 37–42 (2019).

20- Sanville E., Burnin A., and BelBruno J. J., Experimental and Computational Study of Small (n) 1-16) Stoichiometric Zinc and Cadmium Chalcogenide Clusters .*J. Phys. Chem. A*, 110, 2378-2386(2006).

21- "Gaussian 09" Revision E.01, Frisch M.J., et al Cioslowski J. ,Fox D.J., *Gaussian, Inc., Wallingford CT*, (2009).

22- Gouma P. I., Nanomaterials for chemical sensors and biotechnology. *Pan Stanford Publishing, Pte. Ltd*., (2010).

23- Buschow K.h.J., handbook of magnetic materials. 16, *Elsevier*, B.V. (2006).

24- Sharma S., Malik M. A., Chandel T., Thakur V. and Rajaram P., Growth and Characterization of ZnSe Nanoparticles. *AIP Conf. Proc*., 1591, 474-476 (2014).

25- Hedayati K., Zendehnam A. and Hassanpour F., Fabrication and Characterization of Zinc Sulfide Nanoparticles and Nanocomposites Prepared via

a Simple Chemical Precipitation Method. *J., Nanostruct* 6, 3. 207-212 (2016).

26- Hammes G. G. ,Spectroscopy for the biological sciences. *Hoboken, N. J: Wiley*, (2005).

27- Kumar P., Singh J., Pandey M. K., Jeyanthi C.E., Siddheswaran R., Paulraj M., Hui K.N., and Hui K.S., Synthesis, structural, optical and Raman studies of pure and lanthanum doped ZnSe nanoparticles. *Materials Research Bulletin*, 49, 144–150 (2014).

28- Stroyuk A. L., Raevskaya A. E., Korzhak A. V. and Kuchmii S. Y. ,Zinc sulfide nanoparticles: Spectral properties and photocatalytic activity in metals reduction reactions. *Journal of Nanoparticle Research*, 9, 1027–1039 (2007).

تحليل الأطياف الإلكترونية ،رامان و UV-vis للتراكيب $Zn_{11}S_{11}$,$Zn_{11}Se_{11}$ والسبائك الثلاثية $Zn_{11}S_nSe_{11-n}$(n= 1-11) دراسة باستخدام A DFT/TDDFT

حسين حاكم عبد[a*]، حيدر محمد عبد الجليل [a] ، مضر احمد عبد الستار[b]

[a]قسم الفيزياء، كلية العلوم، جامعة بابل، العراق

[b]وزارة العلوم والتكنولوجيا، بغداد، العراق

الخلاصة

$Zn_{11}S_{11}$,$Zn_{11}Se_{11}$ والسبائك الثلاثية المتكونة من $Zn_{11}S_nSe_{11-n}$ (n = 1 - 11) ذات التركيب المكعب المتمثل بالتركيب النانوي المسمى تترامنتان، درست نظريا بقياس الخصائص الكترونية، وأطياف رامان والأطياف ضمن المدى الفوق بنفسجي-والمرئي. ومستويات LUMO و HOMOلوحظت أنها تتغير مع عدد ذرات الكبريت. فجوة الطاقة للمركب $Zn_{11}Se_{11}$ (2.377205 eV) تزداد مع زيادة ذرات الكبريت.
$Zn_{11}S_8Se_3$ لها فجوة طاقة (3.061305 eV) أقل من بقية السبائك. فجوة الطاقة المحسوبة للمركب$Zn_{11}S_{11}$ (3.597374 eV) في تطابق عالي مع القيمة التجريبية (3.6 eV). أطياف رامان للسبائك الثلاثية $Zn_{11}S_nSe_{11-n}$ تحتوي على قمم ناتجة من الترابط ($Zn_{11}Se_{11}$+$Zn_{11}S_{11}$).
$Zn_{11}Se_{11}$ تمتلك قمة عند $260.42\ cm^{-1}$ مزاحة عن القيم التجريبية بانحراف صغير ناتج عن التأثير الكمي .
أطياف UV-vis للسبائك الثلاثية انحرفت باتجاه مستوي الطاقة العالي مع زيادة عدد ذرات الكبريت وتقترب تدريجا من طيف $Zn_{11}S_{11}$ ما عدا $Zn_{11}S_8Se_3$ تمتلكλ_{max} عند 342 nm. هذه التراكيب النانوية مناسبة للاستخدام في مجالات مختلفة مثل العدسات ،الأجهزة الكتر وضوئية ،الطاقة الشمسية والمتحسسات البايولوجية.كل النتائج أجريت باستخدام نظرية دالية الكثافة المعتمدة وغير المعتمدة على الزمن عند المستوي B3LYP ودالة أساس SDD وباستخدام برنامج الكاوسين ٠٩.